Monthly Notices
of the
ROYAL ASTRONOMICAL SOCIETY

MNRAS **438,** 1784–1793 (2014)
Advance Access publication 2014 January 2

doi:10.1093/mnras/stt2317

Interacting galaxies: corotating and counter-rotating systems with tidal tails

Valeria Mesa,[1,2]★ Fernanda Duplancic,[1,3] Sol Alonso,[1,3] Georgina Coldwell[1,3] and Diego G. Lambas[1,4]

[1]*Consejo de Investigaciones Científicas y Técnicas (CONICET), Avenida Rivadavia 1917, C1033AAJ, Buenos Aires, Argentina*
[2]*Instituto Argentino de Nivología Glaciología y Ciencias Ambientales (IANIGLA), Parque Gral San Martín, CC 330, CP 5500, Mendoza, Argentina*
[3]*Instituto de Ciencias Astronómicas, de la Tierra y del Espacio (ICATE), CC 49, CP 5400, San Juan, Argentina*
[4]*Instituto de Astronomía Teórica y Experimental (IATE), Observatorio Astronómico, Universidad Nacional de Córdoba, Laprida 854, X5000BGR, Córdoba, Argentina*

Accepted 2013 November 29. Received 2013 November 20; in original form 2013 August 30

ABSTRACT

We analyse interacting galaxy pairs with evidence of tidal features in the Sloan Digital Sky Survey Data Release 7. The pairs were selected within $z < 0.1$ by requiring a projected separation $r_{\rm p} < 50\,h^{-1}$ kpc and relative radial velocity $\Delta V < 500\,{\rm km\,s^{-1}}$. We complete spectroscopic pairs using galaxies with photometric redshifts considering $\Delta V_{\rm phot} < 6800\,{\rm km\,s^{-1}}$, taking into account the mean photometric redshift uncertainty. We classify by visual inspection pairs of spirals into corotating and counter-rotating systems. For a subsample of non-active galactic nucleus (non-AGN) galaxies, counter-rotating pairs have larger star formation rates and a higher fraction of young, star-forming galaxies. These effects are enhanced by restricting to $r_{\rm p} < 12\,h^{-1}$ kpc. The distributions of C, $D_n(4000)$ and $(M_u - M_r)$ for AGN galaxies show that counter-rotating hosts have bluer colours and younger stellar population than the corotating galaxies although the relative fractions of Seyfert, LINER, Composite and Ambiguous AGN are similar. Also, counter-rotating hosts have more powerful AGN as revealed by enhanced Lum[O III] values. The number of corotating systems is approximately twice the number of counter-rotating pairs which could be owed to a more rapid evolution of counter-rotating systems, besides possible different initial conditions of these interacting pairs.

Key words: galaxies: interactions – galaxies: starburst – galaxies: statistics.

1 INTRODUCTION

Galaxy interactions are one of the main mechanisms claimed for inducing star formation (Yee & Ellingson 1995; Kennicutt 1998), where starbursts are fuelled by gas inflows produced by the tidal torques generated during the encounters. Barton, Geller & Kenyon (2000) and Lambas et al. (2003) performed statistical analysis of star formation activity of galaxy pairs showing that proximity in radial velocity and projected distance is correlated with an increase in the star formation activity. Alonso et al. (2006) analyse close pairs and found an excess of blue galaxies with respect to the control sample and associate this phenomenon with a larger fraction of star-forming galaxies. They also found that in close pairs, there is an increment in the fraction of red galaxies compared to systems without a near companion. The authors propose a scenario where galaxies in pairs have formed stars efficiently at early stages of their evolution; therefore, at present, they exhibit red colours. Another interpretation is that the presence of dust stirred up during encounters could affect colours and, probably, partially obscure the star formation activity. Pérez et al. (2009) analysed the colour distribution of close galaxy pairs finding an excess in both red and blue tails with respect to control samples. They also found that the trends still persist even after removing possible bias effects in the control sample selection. These results reinforce the claim that the excesses of blue and red galaxies are actually produced by galaxy interactions and not introduced by a biased selection.

Alonso et al. (2012) performed an analysis of close galaxy pairs in groups and clusters, finding that these pairs tend to reside in groups with low-density global environments. The authors also showed that pair galaxies have a significant excess of young stellar population with respect to group member galaxies without near companion. Recently, Lambas et al. (2012, hereafter L12) stressed the importance of studying different types of interactions and they classified pair galaxies into three categories: pairs undergoing merging (M), pairs with evident tidal features (T) and non-disturbed pairs (N). They also found an excess of galaxies in the blue peak in M systems, while T pairs show a larger fraction of galaxies in the red peak, compared to N systems, especially for minor interactions. These results suggest that the variation of the blue and red peak locations of

★ E-mail: vmesa@mendoza-conicet.gob.ar

the colour bimodal distribution could be driven by different aspects of galaxy interactions such as evolutionary stage, gas content, interaction strength, etc. In particular, L12 highlight the contribution of tidal interactions to the read peak in the galaxy pair colour distribution. Therefore, it is interesting to focus on tidal interactions in order to analyse the role of this special type of encounters on the main properties of galaxies in interacting systems.

Tidal interactions in galaxy pairs can produce several morphological features that are short lived such as extended structures, bridges and tidal tails. Observations indicate that the probability to have grand-design arms is much higher for galaxies in binaries or groups than in the field (Kormendy & Norman 1979). Reshetnikov & Sotnikova (2001) and references therein show that the local fraction of tailed objects is about 1–2 per cent of the local galaxy population, and that the size of the tidal tails is related to the global dynamical structure of the interacting galaxies. Mohamed et al. (2011) point out that the tails in distant galaxies are shorter than those in nearby ones, reflecting the evolution with redshift of the sizes of spiral galaxies and their tidal structures. They also show that in simulated galaxies with low-mass haloes, tidal tails turn out to be very long and the interacting galaxies merge very rapidly. Besides many authors have found objects such as dwarf galaxies and globular clusters in tidal debris from galaxy interactions (Mirabel, Dottori & Lutz 1992; Hunsberger, Charlton & Zaritsky 1996; Charlton et al. 2000; Smith et al. 2010).

In this work, we present an analysis of the galaxy properties in tidal interacting pairs, considering different types of morphological features that show this special type of systems. This paper is structured as follows. Section 2 describes the data used in this work. In Section 3, we show the procedure used to construct the tidal interacting pair catalogue, explaining the classification process of tidal pair galaxies, and we also present the general properties of the catalogue. An analysis of star formation rates (SFR), colours and stellar population, and their dependence on the different classifications in our sample of tidal interactions is described in Section 4. In addition, host active galaxy properties and nuclear activity are analysed in this section. Finally in Section 5, we summarize our main conclusions.

Throughout this paper, we adopt a cosmological model characterized by the parameters $\Omega_{\rm m} = 0.3$, $\Omega_{\Lambda} = 0.7$ and $H_0 = 100\,{\rm km\,s^{-1}\,Mpc^{-1}}$.

2 DATA

Data Release 7 of Sloan Digital Sky Survey (SDSS-DR7; York et al. 2000; Abazajian et al. 2009) is the seventh major data release, corresponding to the completion of the survey SDSS-II. It comprises 11.663 square degrees of imaging data, with an increment of ∼2000 square degrees, over the previous data release, mostly in regions of low Galactic latitude. SDSS-DR7 provides imaging data for 357 million distinct objects in five bands, *ugriz*, as well as spectroscopy over $\simeq \pi$ steradians in the North Galactic cap and 250 square degrees in the South Galactic cap. The average wavelengths corresponding to the five broad-bands are 3551, 4686, 6165, 7481 and 8931 Å (Fukugita et al. 1996; Hogg et al. 2001; Smith et al. 2002). For details regarding the SDSS camera, see Gunn et al. (1998); for astrometric calibrations, see Pier et al. (2003). The survey has spectroscopy over 9380 square degrees; the spectroscopy is now complete over a large contiguous area of the Northern Galactic cap, closing the gap that was present in previous data releases.

In this work, we analyse spectroscopic and photometric data extracted from SDSS-DR7. The spectroscopic data were derived from the main galaxy sample (MGS; Strauss et al. 2002) obtained from the `fits` files at the SDSS home page.[1] For this sample, *k*-corrections band-shifted to $z = 0.1$ were calculated using the software K-CORRECT_V4.2 of Blanton & Roweis (2007). The photometric data were derived from the photometric catalogue constructed by O'Mill et al. (2011).[2] These authors compute photometric redshift and *k*-correction for the photometric data of the SDSS-DR7. The rms of the photometric redshift is $\sigma_{\rm phot} \sim 0.0227$, and *k*-corrections were obtained through joint parametrization of redshift and reference frame (at $z = 0.1$) $(g - r)$ colour. For both data sets, *k*-corrected absolute magnitudes were calculated from Petrosian apparent magnitudes converted to the AB system.

3 INTERACTING PAIR GALAXIES

Galaxies in tidal pairs are subject to diverse perturbations that may alter their morphology and generate peculiar features such as bridges and tails. This diversity of structures can be produced by differences in the internal nature of the galaxies in the tidal pair interactions. For this reason, the aim of this section is to present a sample of tidal pairs in order to explore the different types of such interactions.

3.1 Spectroscopic galaxy pair catalogue

Some recent statistical work focus on the construction of galaxy pair catalogues with different projected separation ($r_{\rm p}$) and relative radial velocity limits (ΔV). Lambas et al. (2003) found that galaxies with a close companion within $r_{\rm p} < 25\,h^{-1}$ kpc and $\Delta V < 100\,{\rm km\,s^{-1}}$ showed a higher star formation activity than isolated galaxies with similar redshift and luminosity distributions. Ellison et al. (2010), in a study of the effects of environment on interactions, constructed a sample of pairs with $r_{\rm p} < 80\,h^{-1}$ kpc and $\Delta V < 500\,{\rm km\,s^{-1}}$ selected from SDSS-DR4, finding that pairs in high-density environments are characterized by wider separations and larger values of ΔV. More recently, Scudder et al. (2012) presented a sample of pairs from SDSS-DR7 with relative projected separation $r_{\rm p} < 80\,h^{-1}$ kpc and relative radial velocities $\Delta V < 300\,{\rm km\,s^{-1}}$. These pairs show SFR enhancements of 30 per cent out to at least $80\,h^{-1}$ kpc.

In our previous work (L12), we build a catalogue of 1959 galaxy pairs with projected separation $r_{\rm p} < 25\,h^{-1}$ kpc and relative radial velocities $\Delta V < 350\,{\rm km\,s^{-1}}$, within $z < 0.1$, finding 589 pairs that show tidal features. In order to obtain a larger number of pairs, and therefore improve the statistics, we extended this sample to $r_{\rm p} < 50\,h^{-1}$ kpc and $\Delta V < 500\,{\rm km\,s^{-1}}$, and consider pairs with $z < 0.1$, where z is the redshift of the brightest galaxy member of the system. In this way, we obtain a sample of 1283 pair galaxies with tidal signatures.

We performed an eye-ball classification using the SDSS-DR7 imaging available in CasJobs[3] in order to distinguish between different classes of tidal interactions. We classified the sample taking into account the presence of either large-scale tidal tails (Tt) or a connecting bridge (Tb). Thus, Tt types are either pairs of two spiral galaxies or composed of a spiral and an elliptical galaxy while most Tb systems consist of a pair of elliptical galaxies connected by a bridge. We found that 85 per cent of the pairs were classified into these subsamples. The remaining pairs that do not fulfil these two

[1] http://www.sdss.org/dr7/products/spectra/getspectra.html
[2] http://casjobs.starlight.ufsc.br/casjobs/
[3] http://cas.sdss.org/astrodr7/

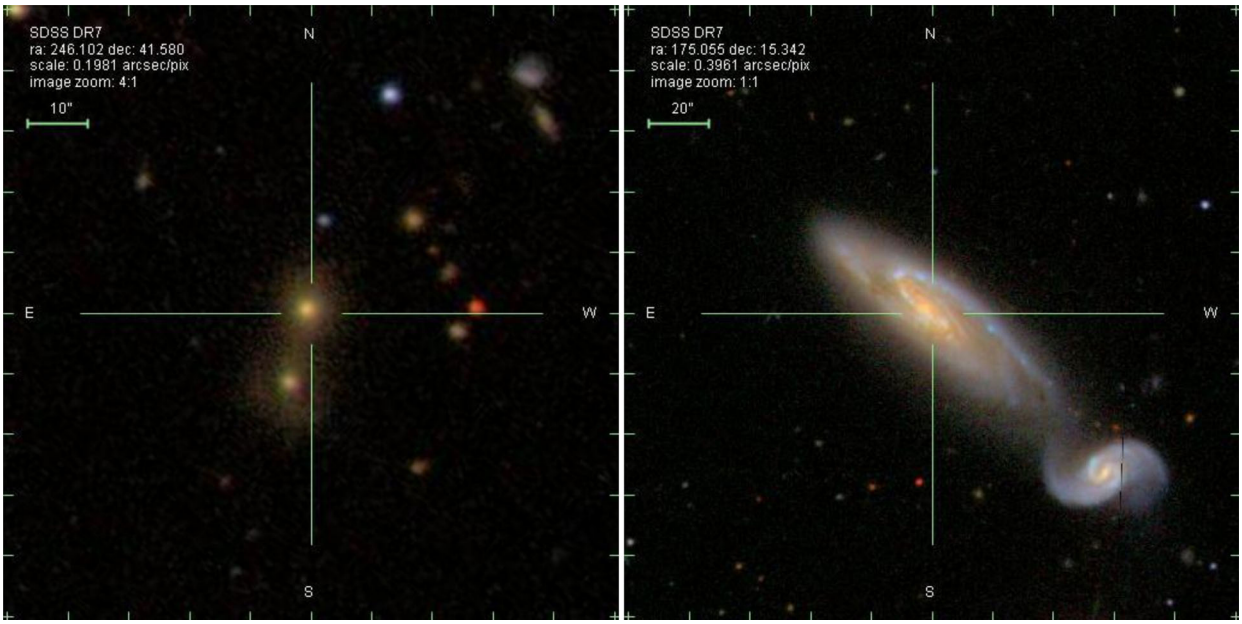

Figure 1. Examples of tidal galaxy pair images. Left: galaxy pairs with a bridge (Tb). Right: interactions with tidal tails (Tt).

categories were excluded from the present analysis. Fig. 1 shows examples of Tt and Tb pairs. The visual inspection of the pairs was performed by all the authors dividing the total sample into subsamples of similar number of pairs. The reliability of the classification was addressed by a comparison of the classification of all authors in a common subsample. This comparison provides a classification uncertainty which we estimate to be approximately 3 per cent.

Under these considerations, the resulting spectroscopic tidal galaxy pair catalogue comprises a total of 1082 pairs.

3.2 Spectrophotometric galaxy pair catalogue

The SDSS spectrograph uses fibres manually connected to plates in the telescope's focal plane. These fibres are mapped through a mosaic algorithm (Blanton et al. 2003) that optimizes the observation of large-scale structures. Two fibres cannot be placed closer than 55 arcsec (Strauss et al. 2002), so for two objects with the same priority (such as two MGS galaxies) and whose centres are closer than 55 arcsec, the algorithm selects at random the galaxy which will be observed spectroscopically. There are regions where the plates overlap (about 30 per cent of the mosaic regions), in which both objects may be observed. Due to fibre collision the spectroscopic sample is affected by incompleteness. The magnitude limit of spectroscopic objects is $r = 17.77$, but not all galaxies brighter than this limit were observed. This issue becomes more important when analysing compact objects.

Recently, O'Mill et al. (2012) employed photometric redshift information to quantify this effect on the detection of triplets of galaxies in the SDSS-DR7. These authors conclude that photometric redshift provides very useful information, allowing them to assess fibre collision incompleteness and complete the sample of triple systems at low redshift.

In order to recover pair systems lost due to the fibre collision effect, we have included galaxies with photometric redshifts that have r-band magnitude $r < 17.77$. For each galaxy with spectroscopic measurements in the redshift range $z < 0.1$, we have searched a photometric companion that has a projected distance $r_p < 50\,h^{-1}$ kpc and a relative radial velocity $\Delta V_{\rm phot} < 6800\,{\rm km\,s^{-1}}$; the latter value corresponds to $c \times \sigma_{\rm phot}$, where $\sigma_{\rm phot}$ is the mean photometric redshift error and c is the speed of light. O'Mill et al. (2012) found that the $1\sigma_{\rm phot}$ interval provides a suitable compromise between high completeness and low contamination in the detection of triplets of galaxies. Including photometric information allows us to increment the number of galaxies in the sample under analysis and, therefore, improve the statistical significance of our results.

Table 1. Number of Tt and Tb pairs in the spectroscopic and spectrophotometric tidal pair samples.

Samples	Spectroscopic	Spectrophotometric	Total
Tt	525	944	1469
Tb	557	637	1194
Total	1082	1581	2663

Similarly to the spectroscopic catalogue, we perform an eyeball classification of this sample, finding 2043 spectrophotometric galaxy pairs with tidal signs. Apart from the restriction on $\Delta V_{\rm phot}$, the existence of tidal signatures reinforces that the galaxy pairs in the spectrophotometric sample are physical systems. About 78 per cent of the pairs in this sample were classified as Tt or Tb; the remaining pairs that do not fulfil these two categories were excluded from the analysis. The resulting spectrophotometric tidal galaxy pair catalogue comprises a total of 1581 pairs.

Table 1 provides the classification and number of pairs in the spectroscopic and spectrophotometric tidal pair samples.

3.3 Characteristics of the pair samples

In order to analyse different physical properties of galaxies in tidal pairs, we select galaxies with spectroscopic measurements and cross-correlate them with the derived galaxy properties from the Max Planck Institute for Astrophysics & Johns Hopkins University (MPA-JHU Group) emission-line analysis for the SDSS-R7.[4] From

[4] Available at http://www.mpa-garching.mpg.de/SDSS/DR7/

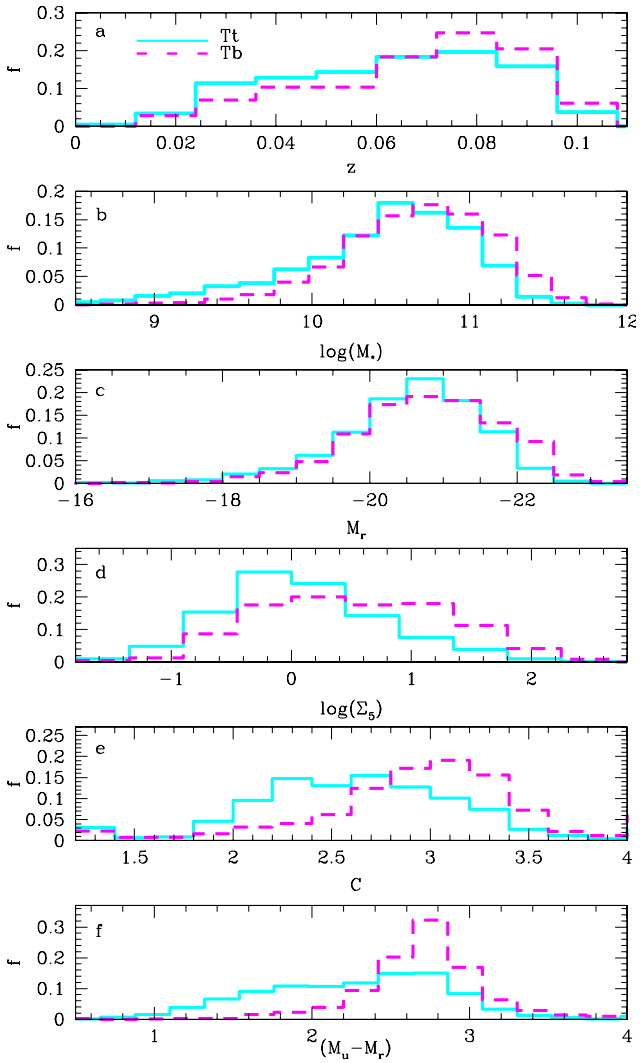

Figure 2. From top to bottom, (a) distribution of z, (b) $\log(M_*)$, (c) M_r, (d) $\log(\Sigma_5)$, (e) C and (f) $(M_u - M_r)$ for galaxies in pairs classified as Tt (solid lines) and for Tb (dashed lines).

this catalogue, we use the star formation rate normalized to the total mass in stars, $\log(\mathrm{SFR}/M_*)$, taken from Brinchmann et al. (2004). We also use the spectral index $D_n(4000)$, as an indicator of the age of stellar populations. This spectral discontinuity occurring at 4000 Å (Kauffmann, White & Guiderdoni 2002) arises by an accumulation of a large number of spectral lines in a narrow region of the spectrum, an effect that is important in the spectra of old stars. We have adopted the Balogh et al. (1999) definition of $D_n(4000)$ as the ratio of the average flux densities in the narrow continuum bands (3850–3950 Å and 4000–4100 Å). We also use total stellar masses (M_*) based on fits to the photometry (Salim et al. 2007).

In Fig. 2, we show different properties of Tt and Tb galaxy pair interactions (redshift, z, stellar mass content, M_*, absolute r-band magnitude, M_r, local density parameter, Σ_5, concentration index, C and $(M_u - M_r)$ colour). From the upper panel, it can be appreciated that both samples expand similar z ranges but the Tb pairs show a distribution slightly shifted towards higher z values. From panel (b), we find that the Tb pairs show a stellar mass distribution with small shift towards larger $\log(M_*)$ values, than galaxies in the Tt sample. This behaviour is also reflected in the M_r distribution (see panel c).

With the purpose of analysing the local density environment of the galaxy pairs in our samples, we have calculated the local density parameter Σ_5, to give an estimate of the mean environment of the two subsamples. This parameter is defined through the projected distance d to the fifth nearest neighbour brighter than $M_r < -20.5$ (Balogh et al. 2004), $\Sigma_5 = 5/(\pi d^2)$, with a radial velocity difference less than 1000 km s^{-1}, and provides a suitable measurement of the local density of the systems. Alonso et al. (2006) identified three regions according to the value of $\log(\Sigma_5)$: low density ($\log(\Sigma_5) < -0.57$), medium density ($-0.57 < \log(\Sigma_5) < 0.05$) and high density ($\log(\Sigma_5) > 0.05$). The results displayed in Fig. 2(d) show that Tb pairs present a higher fraction of galaxies residing in high-density environments, while galaxies in Tt pairs are preferentially hosted in environments with intermediate densities.

The concentration index C[5] is a good morphological classification parameter (Strateva et al. 2001) and correlates with the stellar mass (M_*) and SFR (Deng 2013). Yamauchi et al. (2005) performed a galaxy morphological classification using the C parameter, finding very good agreement with the visual classification. We adopted the critical concentration index value of $C = 2.5$ to segregate concentrated, bulge-like galaxies ($C > 2.5$) and more extended, disc-like objects ($C < 2.5$). C index distributions are showed in panel (e) of Fig. 2. From this figure, it can be appreciated that the sample of Tb pairs exhibit higher values of C index with respect to the Tt sample. Moreover, we find that Tb pairs show a higher fraction of galaxies with $C > 2.5$ (≈85 per cent), with respect to the Tt sample (≈60 per cent). This result indicates that a higher fraction of galaxies in the Tb sample presents bulge morphology, while Tt pairs show a significant fraction of disc-type objects. This result is expected under the classification scheme used in this work and because elliptical galaxies are more compact and tend to inhabit higher density regions, so under these conditions it is more difficult to develop tidal tails.

Nevertheless, the most significant difference between galaxies in Tb and Tt pairs resides in the $(M_u - M_r)$ colour distribution. About 95 per cent of the Tb galaxies present red colours ($(M_u - M_r) > 2.0$) while galaxies in Tt pairs present a more uniform distribution, with 68 per cent of galaxies with redder colours. This result is consistent with the previously found in the distribution of the concentration index, indicating that the sample of Tb pairs is composed mostly of redder early-type galaxies.

The trends found with this analysis persist even when considering control samples matched in z, M_r, M_* and Σ_5. This result suggests that the so-called red peak present in the colour distribution of pair galaxies, reported by different authors (e.g. Alonso et al. 2006, 2012; Pérez et al. 2009; Darg et al. 2010; Patton et al. 2011), is mostly populated by this special type of tidal interaction that comprises galaxies with a bridge (Tb). We will analyse this topic in detail in a forthcoming paper and, in what follows, we will consider only interactions with tidal tails (Tt) and in particular we will study the interactions between spiral galaxies within this subsample.

4 COROTATING AND COUNTER-ROTATING SYSTEMS

Numerical simulations show that prograde encounters between equal-mass galaxies represent the most favourable scenario for creating tidal tails (Toomre & Toomre 1972; Dubinski, Mihos & Hernquist 1996); instead, retrograde encounters have greater star

[5] $C = r90/r50$ is the ratio of Petrosian 90–50 per cent r-band light radii.

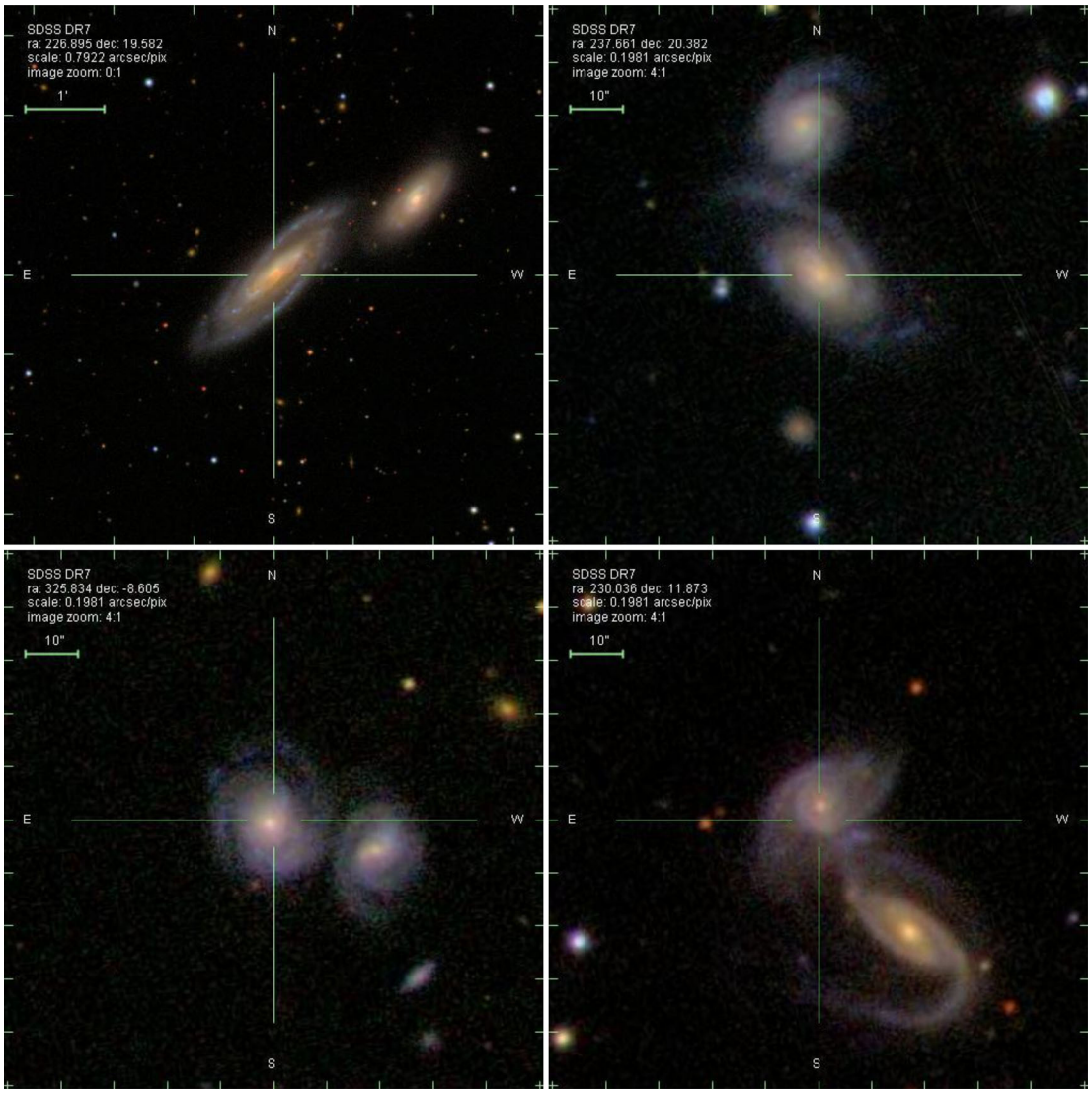

Figure 3. Examples of galaxy pair images with different classification: corotating (left) and counter-rotating (right) in the spectroscopic sample (upper panels) and spectrophotometric catalogue (bottom panels).

formation efficiency than direct encounters. Di Matteo et al. (2007) analysed direct and retrograde galaxy encounters finding that galaxies with opposite angular momentum (retrograde encounters) are less affected by tidal interactions and the gas mass content remains confined in the disc forming a reservoir for the intense starburst in the final stage of the merging. On the other hand, Cervantes-Sodi, Hernandez & Park (2010) found a correlation for the spin magnitude of neighbouring galaxies, but no clear alignment of orientation. Regarding halo masses, Dubinski et al. (1996) found that it is difficult to form a long tail in collisions of galaxies with very massive haloes.

In the following study, we only analyse tidal interactions between spiral galaxies with tidal tails within Tt pairs, and we visually subclassified these pairs according to the sense of rotation of the spiral arms. Therefore, we have defined two categories: corotating and counter-rotating pairs. If both galaxies have the same spiral pattern sense, we call the system corotating, and otherwise we call the system counter-rotating. Analogously to Section 3.1, we estimate the uncertainty in this classification that results in 4 per cent. It is noteworthy that the visual inspection performed in order to identify the sense of rotation of the galaxy spiral arms produces a selection effect and, therefore, most of the systems under study in this section are major mergers. We have analysed how these different spin configurations affect galaxy luminosities, SFR, spectral indicators of stellar populations, colours and active nucleus properties.

The upper panels of Fig. 3 show images of typical examples of corotating and counter-rotating pairs in the spectroscopic sample. In a similar way, the bottom panels show images of typical examples of these categories in the spectrophotometric catalogue.

Table 2 provides the percentages of corotating and counter-rotating pairs in the spectroscopic and spectrophotometric samples. Remarkably, we find that corotating systems double the number of the counter-rotating pairs. A possible explanation for this fact could reside in the initial conditions of nearby haloes and that counter-rotating interactions are likely to be more violent, with mergers occurring faster, and with less prominent large-scale tails (Hernandez & Lee 2004). We notice that this effect is present in both samples, spectroscopic and spectrophotometric catalogues, indicating that the results are not biased by the inclusion of photometric galaxies.

Table 2. Classification, number of pairs and percentages of corotating and counter-rotating galaxy pairs in the spectroscopic and spectrophotometric samples (top and bottom, respectively).

Sample	Classification	Number of pairs	Percentages
Spectroscopic	Corotating	171	65.4 per cent
	Counter-rotating	85	34.3 per cent
	Total	256	100 per cent
Spectrophotometric	Corotating	266	66.8 per cent
	Counter-rotating	139	33.2 per cent
	Total	405	100 per cent

4.1 Galaxies without nuclear activity and AGN hosts

In the following analysis, we used galaxies with spectroscopic measurements and distinguish between active galactic nuclei (AGN) and galaxies without a detected AGN (hereafter non-AGN galaxies) in co- and counter-rotating pairs. For the AGN selection, we use the publicly available SDSS emission-line fluxes. The method for emission-line measurement is detailed in Tremonti et al. (2004). Additionally, we have corrected the emission-line fluxes for optical reddening using the Balmer decrement and the Calzetti et al. (2000) dust curve. We assume $R_V = A_V/E(B-V) = 3.1$ and an intrinsic Balmer decrement $(H\alpha/H\beta)_0 = 3.1$ (Osterbrock & Miller 1989). Since the true uncertainties in the emission-line measurements were underestimated, the signal-to-noise ratio (S/N) of every line was calculated with the emission-line flux errors adjusted according to the uncertainties suggested by the MPA/JHU catalogue.

The AGN galaxy sample was selected using a standard diagnostic diagram proposed by Baldwin, Phillips & Terlevich (1981, hereafter BPT). This diagram allows the separation of type 2 AGN, from normal star-forming galaxies, using emission-line ratios and depending on their position in the diagram. Furthermore, we used only galaxies with S/N > 2 for all the lines intervening in the diagnostic diagram used to discriminate AGN from H II galaxies. This S/N cut was selected taking into account that the adjusted uncertainties almost duplicated the original errors. So, taking into account the relation between spectral lines, [O III] λ5007, Hβ, [N II] λ6583 and Hα, within the BPT diagram we follow the Kauffmann et al. (2003b) criterion to select type 2 AGN as those with

$$\log_{10}([\mathrm{O\,III}]/\mathrm{H}\beta) > 0.61/(\log_{10}([\mathrm{N\,II}/\mathrm{H}\alpha]) - 0.05) + 1.3; \qquad (1)$$

using this criteria we build two catalogues, a sample of galaxies free of AGN and a sample of AGN galaxies. Under these restrictions, and from a total of 917 interacting galaxies with these spectroscopic measurements, we found 297 AGN, representing a fraction of about 30 per cent. Table 3 summarizes the percentages. It is important to highlight that the percentages of co- and counter-rotating systems

Table 3. Classification, number of galaxies and percentages of corotating and counter-rotating galaxy pairs in the AGN sample (top) and in the galaxy sample (bottom).

Sample	Classification	Number of galaxies	Percentages
AGN	Corotating	191	64.3 per cent
	Counter-rotating	106	35.7 per cent
	Total	297	100 per cent
Non-AGN galaxies	Corotating	417	67.3 per cent
	Counter-rotating	203	32.7 per cent
	Total	620	100 per cent

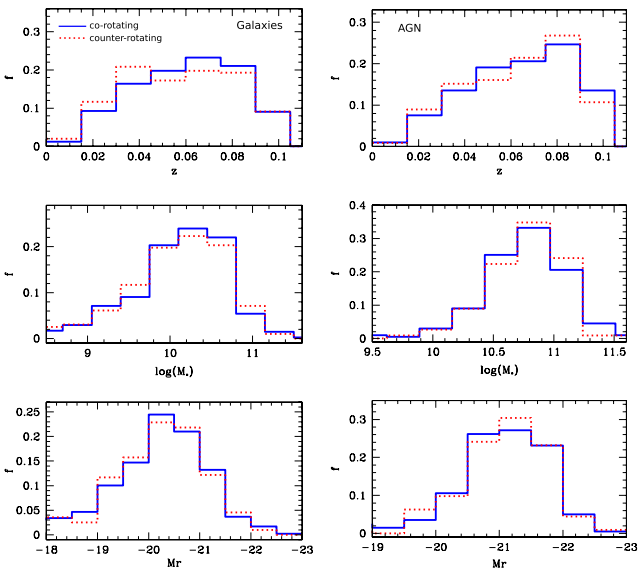

Figure 4. Distribution of redshift (top), absolute r-band magnitude (middle) and stellar mass content (bottom) for the non-AGN galaxy sample (left) and for the AGN galaxy sample (right) in co- and counter-rotating pairs. The solid lines correspond to the corotating and the dotted lines correspond to the counter-rotating galaxy pairs, respectively.

in the sample of non-AGN galaxies and in the sample of AGN are similar.

In Fig. 4, we show the distribution of redshift, stellar mass content and r-band absolute magnitude for the sample of non-AGN galaxies (left) and for the sample of AGN galaxies (right) in co- and counter-rotating pairs (solid and dotted lines, respectively). From this figure, it can be appreciated that both samples present similar z, M_* and M_r distributions.

4.1.1 Galaxy properties

In this section, we focus our analysis on the sample of spiral galaxies with tidal tails in order to investigate the differences in the properties of the systems according to the sense of rotation of the member galaxy pairs. We study the sample of non-AGN galaxies, defined in the previous subsection, and analyse separately corotating and counter-rotating interactions and their effects on the galaxy properties. We also analyse a subsample of closer encounters considering pairs with projected separations $r_\mathrm{p} < 12\,h^{-1}$ kpc. This value corresponds to the median of the r_p distribution for the total sample.

We analyse the specific star formation rate, SFR/M_*, the $D_n(4000)$ parameter, the $(M_u - M_r)$ colour index and the concentration parameter C.

The distribution of these parameters is shown in Fig. 5 for the two samples with $r_\mathrm{p} < 50\,h^{-1}$ kpc (left) and $r_\mathrm{p} < 12\,h^{-1}$ kpc (right). From this figure, it can be appreciated that the counter-rotating systems show a higher SFR. This effect is more strongly seen in the sample with $r_\mathrm{p} < 12\,h^{-1}$ kpc, where the effect is also reflected in the lower values of the $D_n(4000)$ parameter and $(M_u - M_r)$ colours. Both samples present similar C values.

In order to quantify these differences, we have estimated the fraction of galaxies with $\log(\mathrm{SFR}/M_*) > -10.0$, $D_n(4000) < 1.4$, $(M_u - M_r) < 2.0$ and $C < 2.5$. In Table 4, we summarize these results. All the uncertainties in this paper were derived through a bootstrap resampling technique (Efron 1979). A larger SFR with an associated younger stellar population in counter-rotating systems

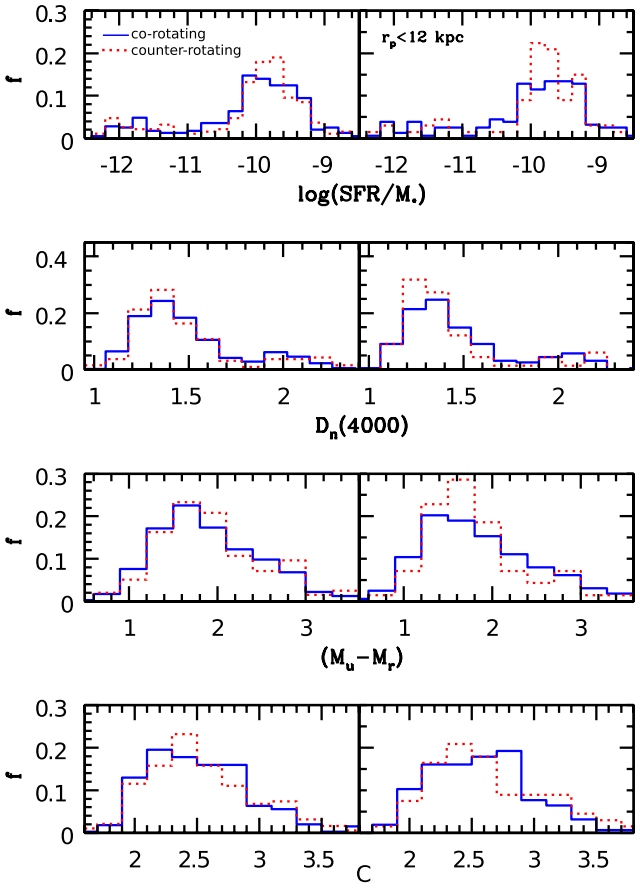

Figure 5. Distribution of $\log(\mathrm{SFR}/M_*)$, $D_n(4000)$, $(M_u - M_r)$ and C for pair galaxies, excluding AGN, classified as co- and counter-rotating (solid and dotted lines, respectively).

can be seen, an effect that is stronger for the closest $r_\mathrm{p} < 12\,h^{-1}$ kpc subsample, with a significance of $\sim 2.5\sigma$. We argue that this larger star formation activity in counter-rotating systems can be related to the larger disturbing effects of such interactions in comparison to those in corotating pairs. According to simulations of disc-type galaxy interactions, there is a tight correlation between the starburst and the pericentre passage (Mihos & Hernquist 1994; Di Matteo et al. 2007). Statistically, low r_p values could have a larger chance of having galaxies at the pericentre distance, giving rise to the stronger effects for the $r_\mathrm{p} < 12\,h^{-1}$ kpc subsample.

4.1.2 AGN and host properties

In this section, we use the sample of AGN described in Section 4.1, with the purpose of analysing the possible differences in the properties of AGN hosts in co- and counter-rotating tidal galaxy pairs. We also investigate the influence of the sense of rotation of tidal interacting spiral galaxies on the black hole activity.

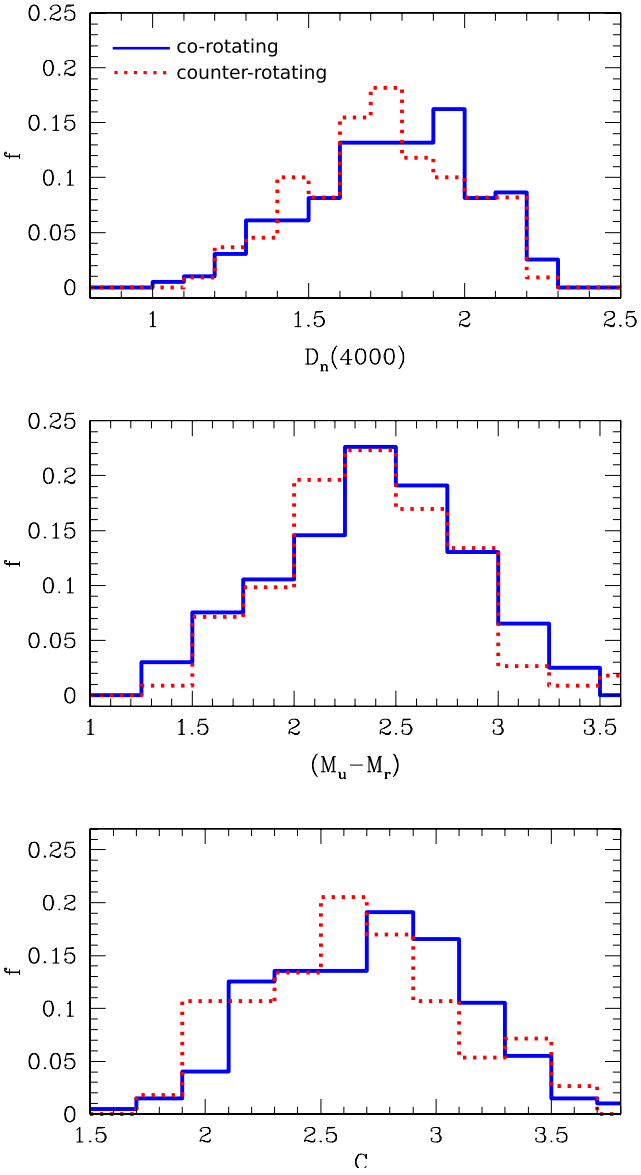

Figure 6. Distribution of C, $D_n(4000)$ and $(M_u - M_r)$ for AGN pair galaxies classified as co- and counter-rotating (solid and dotted lines, respectively).

In Fig. 6, we show the distribution of C, $D_n(4000)$ and $(M_u - M_r)$ colour for co- and counter-rotating AGN host galaxies. This figure shows only a slightly difference in the behaviour of AGN hosts for the two subsamples, with counter-rotating galaxies presenting

Table 4. Percentages of galaxies with $\log(\mathrm{SFR}/M_*) > -10.0$, $D_n(4000) < 1.4$, $(M_u - M_r) < 2.0$ and $C < 2.5$ in corotating and counter-rotating systems.

	Pairs with $r_\mathrm{p} < 50\,h^{-1}$ kpc		Pairs with $r_\mathrm{p} < 12\,h^{-1}$ kpc	
Ranges	Corotating per cent	Counter-rotating per cent	Corotating per cent	Counter-rotating per cent
$\log(\mathrm{SFR}/M_*) > -10.0$	52.7 ± 2.5	59.0 ± 3.4	57.3 ± 3.8	72.2 ± 5.5
$D_n(4000) < 1.4$	49.92 ± 2.6	55.4 ± 3.5	54.7 ± 3.9	68.0 ± 5.5
$(M_u - M_r) < 2.0$	62.4 ± 2.4	62.0 ± 3.4	65.4 ± 3.7	72.4 ± 5.4
$C < 2.5$	52.2 ± 2.5	54.0 ± 3.6	46.2 ± 3.8	49.3 ± 6.1

Table 5. Percentages of AGN galaxies with $D_n(4000) < 1.8$, $(M_u - M_r) < 2.3$ and $C < 2.7$ in corotating and counter-rotating hosts.

Ranges	Corotating per cent	Counter-rotating per cent
$D_n(4000) < 1.8$	51.7 ± 3.5	61.1 ± 4.8
$(M_u - M_r) < 2.3$	38.6 ± 3.4	45.9 ± 4.7
$C < 2.7$	45.3 ± 3.5	57.0 ± 4.5

bluer colours and younger stellar population than their corotating counterpart. In order to quantify this difference, we estimate the fraction of galaxies with $D_n(4000) < 1.8$, $(M_u - M_r) < 2.3$ and $C < 2.7$. The thresholds were chosen taking into account that, on average, AGN pairs with tidal features have larger $D_n(4000)$ values and redder colours (Liu, Shen & Strauss 2012). In addition, Deng (2013) showed that AGN are preferentially found in more concentrated host galaxies. The results are shown in Table 5, and similar tendencies as in the galaxy sample analysed in the previous section can be appreciated.

As a tracer of the AGN activity, we focus here on the dust-corrected luminosity of the [O III] λ5007 line, Lum[O III]. This estimator is widely used by several authors (Mulchaey et al. 1994; Kauffmann et al. 2003b; Brinchmann et al. 2004; Heckman et al. 2004, 2005) mainly due to that the [O III] line is one of the strongest narrow emission lines in optically obscured AGN and with very low contamination by contributions of star formation in the host galaxy.

The distributions of the AGN power derived from the O III luminosity of the two subsamples are shown in Fig. 7, and it can be appreciated that counter-rotating AGN galaxies present a slight excess of high log(Lum[O III]) values, with respect to the corotating counterpart. In order to quantify these excesses, we calculate the fraction of galaxies with L[O III] > 6.5 for both samples, finding 21.03 ± 2.92 and 27.71 ± 4.18 per cent for co- and counter-rotating galaxies, respectively. This result could be suggesting that AGN host galaxies in counter-rotating pairs are more powerful than those in the corotating systems.

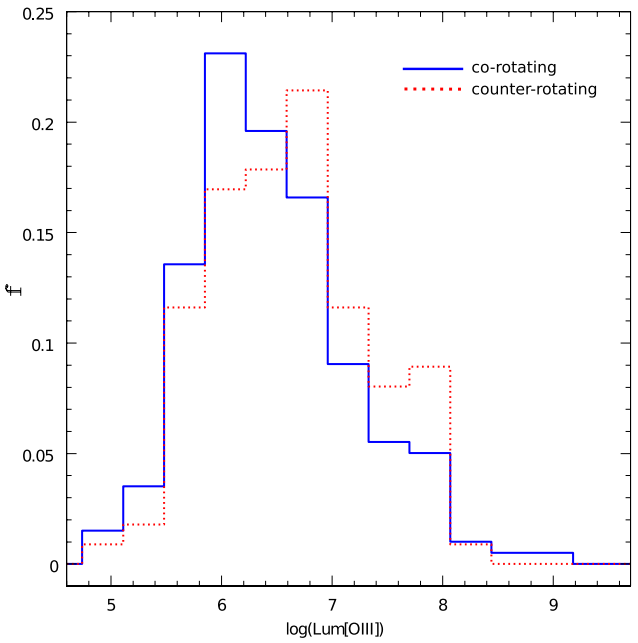

Figure 7. Distribution of log(Lum[O III]) for AGN galaxies classified as corotating (solid lines) and counter-rotating (dotted lines).

Moreover, the AGN sample can be classified into Composite, Seyfert, LINER and Ambiguous following the classification procedure proposed by Kewley et al. (2001, 2006). In this scheme, Kewley et al. (2001) define a theoretical discrimination between starburst regions from objects of other types of excitation using three BPT diagrams, as shown in Fig. 8 (solid lines). Thus, this AGN classification depends on the relative location following equations (2)– (4):

$$\log_{10}([\mathrm{O\,III}]/\mathrm{H}\beta) > 0.61/(\log_{10}([\mathrm{N\,II}]/\mathrm{H}\alpha) - 0.47) + 1.19 \quad (2)$$

$$\log_{10}([\mathrm{O\,III}]/\mathrm{H}\beta) > 0.72/(\log_{10}([\mathrm{S\,II}]/\mathrm{H}\alpha) - 0.32) + 1.30 \quad (3)$$

$$\log_{10}([\mathrm{O\,III}]/\mathrm{H}\beta) > 0.73/(\log_{10}([\mathrm{O\,I}]/\mathrm{H}\alpha) + 0.59) + 1.33. \quad (4)$$

In addition, Kewley et al. (2006) provide an empirical division between Seyfert and LINER galaxies given by the following parametrization, where Seyfert galaxies are located above the Seyfert–LINER line (dashed line in Figs 8b and c) on the S II/Hα and O I/Hα diagrams:

$$\log_{10}([\mathrm{O\,III}]/\mathrm{H}\beta) > 1.89\log_{10}([\mathrm{S\,II}]/\mathrm{H}\alpha]) + 0.76 \quad (5)$$

$$\log_{10}([\mathrm{O\,III}]/\mathrm{H}\beta) > 1.18\log_{10}([\mathrm{O\,I}]/\mathrm{H}\alpha] + 1.30 \quad (6)$$

and LINER galaxies are located below the Seyfert–LINER line:

$$\log_{10}([\mathrm{O\,III}]/\mathrm{H}\beta) < 1.89\log_{10}([\mathrm{S\,II}]/\mathrm{H}\alpha]) + 0.76 \quad (7)$$

$$\log_{10}([\mathrm{O\,III}]/\mathrm{H}\beta) < 1.18\log_{10}([\mathrm{O\,I}]/\mathrm{H}\alpha] + 1.30. \quad (8)$$

Also, galaxies lying in between the Kauffmann et al. (2003b) and Kewley et al. (2001) classification lines are classified as Composite galaxies. These galaxies seem to be in a transition between the H II region and AGN, and probably contain a mixture of metal-rich stellar population plus AGN emission. Finally, Ambiguous galaxies are those classified as one type of object in one BPT and another in the remaining two diagrams. In Fig. 8, the relative position of the AGN in co- and counter-rotating pairs is shown in the three BPT diagnostic diagrams. As can be appreciated, there is no evidence of differences in the position of AGN in co- and counter-rotating pairs regarding this classification scheme.

The results are quantified in columns 2 and 4 of Table 6 where the percentage of co- and counter-rotating galaxy pairs is calculated for every type of object.

In addition, we have explored which of the AGN subclasses present higher median values of Lum[O III]. The results are shown in columns 3 and 5 of Table 6. It can be noticed that galaxies classified as Composite and Ambiguous present noticeable differences between co- and counter-rotating galaxy pairs for median values of Lum[O III] being higher for the counter-rotating ones. The median of Lum[O III] is almost identical (within the estimated errors) for Seyfert and LINER galaxies. This result suggests that these galaxies which have a dubious AGN classification are those which have the strongest differences depending on the sense of rotation. This fact favours the interpretation of the different Lum[O III] values according to the sense of rotation, as differences in the star formation activity rather than the AGN itself. In this sense, Heckman et al. (2004) compute the average contribution of the AGN to the Lum[O III] for a sample of Composite galaxies and the AGN-dominated galaxies taken from SDSS. The results of their work indicate that the Lum[O III] emission from Composite galaxies comes in a range of 50–90 per cent from AGN activity, while for AGN-dominated galaxies, more than 90 per cent of the Lum[O III] comes from AGN

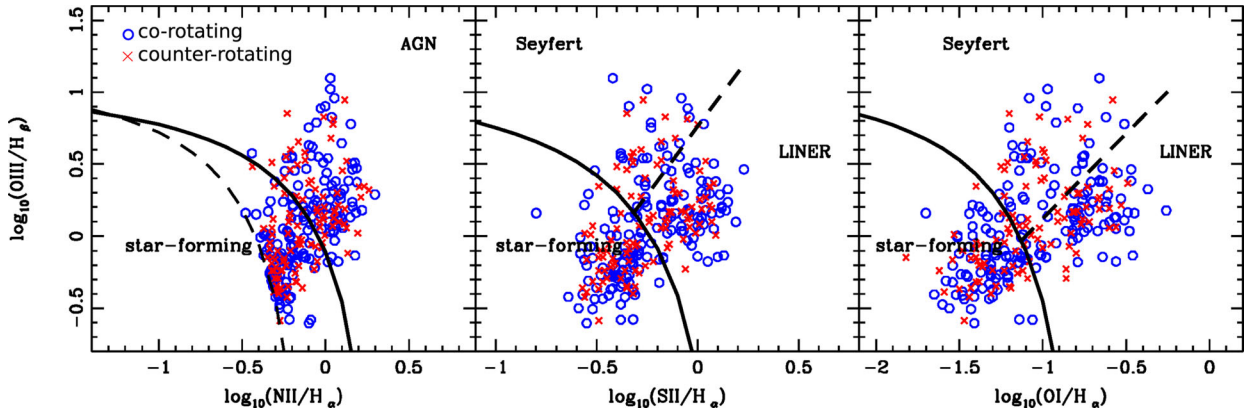

Figure 8. The three BPT diagrams used to classify the emission-line galaxies as: Seyfert, LINER, Composite and Ambiguous galaxies. Left: dashed line shows the Kauffmann et al. (2003a) selection criteria. The Kewley et al. (2006) classification is shown as the solid line. Middle and right: the solid lines separate the star-forming galaxies from the active galaxies and the dashed lines represent the Seyfert–LINER demarcation.

Table 6. Percentages of corotating and counter-rotating AGN galaxies in tidal pairs and median values of (Lum[O III]) for every type of object classification.

	Corotating		Counter-rotating	
Classification	per cent	⟨Lum[O III]⟩	per cent	⟨Lum[O III]⟩
Seyfert	12.9 ± 2.9	7.1 ± 0.4	14.1 ± 3.5	6.9 ± 0.5
LINERs	18.0 ± 3.9	6.1 ± 0.3	19.8 ± 4.4	6.2 ± 0.3
Composite	54.1 ± 7.3	6.4 ± 0.2	50.0 ± 6.9	6.6 ± 0.2
Ambiguous	15.0 ± 3.5	6.2 ± 0.2	16.1 ± 3.8	6.6 ± 0.3

emission. Once nuclear activity is triggered, the corotating versus counter-rotating large-scale structure becomes irrelevant; nuclear activity is controlled by very localized small-scale physics, see for instance Cervantes-Sodi et al. (2011).

5 CONCLUSIONS

We have performed a statistical analysis of interacting pairs with tidal features, selected from SDSS-DR7. We obtained a spectroscopic sample considering $r_p < 50\,h^{-1}$ kpc and $\Delta V < 500\,h^{-1}$ kpc. With the aim to obtain better statistical results, for each galaxy with spectroscopic measurements we have searched a photometric companion with projected distance $r_p < 50\,h^{-1}$ kpc and a radial velocity difference $\Delta V_{phot} < 6810\,\mathrm{km\,s^{-1}}$. First, we divided the sample taking into account the presence of tidal tails (Tt) or a connecting bridge (Tb). These subsamples exhibit similar distributions of z, M_r and $\log(M_*)$, while local environment, concentration index and colour distributions are very different, showing that Tb pairs have a higher fraction of galaxies residing in high-density environments, present redder colours and exhibit a bulge-type morphology. The results found in this analysis persist even when considering control samples matched in z, M_r, M_* and Σ_5, suggesting that the so-called red peak present in the colour distribution of pair galaxies is mostly populated by tidal interaction that comprises galaxies with a bridge (Tb). In this work, we analyse in detail interactions with tidal tails (Tt) between spiral galaxies, and we subclassified these pairs according to the sense of rotation of the spiral arms, by visual inspection of the images. Then, we defined two categories: corotating and counter-rotating pairs.

We can summarize the main results in the following conclusions.

(i) We find that corotating systems double the number of the counter-rotating pairs, an effect that is present in both samples, spectroscopic and spectrophotometric catalogues. This could be due to a combination of parallel spin preference in initial conditions of nearby haloes, a more rapid evolution to merger and a less effective tidal tail development.

(ii) We have studied separately galaxies without nuclear activity, and AGN hosts in co- and counter-rotating tidal pairs. The percentages of co- and counter-rotating tidal systems show the same result as mentioned above in both pair samples. We also find similar distributions of redshift, stellar mass content and r-band absolute magnitude for samples of AGN and non-AGN galaxies in co- and counter-rotating pairs.

(iii) For galaxies with no AGN activity, we find that counter-rotating systems have a higher SFR and a younger stellar population. This effect is stronger in the sample with $r_p < 12\,h^{-1}$ kpc, as expected due to the larger tidal effects associated with closer encounters.

(iv) We find that the distributions of C, $D_n(4000)$ and $(M_u - M_r)$ of AGN host galaxies present a small difference in the behaviour of the two subsamples, showing that counter-rotating hosts have a higher fraction of galaxies with bluer colours and younger stellar population than their corotating counterpart.

(v) The AGN sample was classified into Composite, Seyfert, LINER and Ambiguous following the Kewley et al. (2001, 2006) scheme finding no significant differences in the position of AGN in co- and counter-rotating pairs regarding this classification.

(vi) As a tracer of the AGN activity, we analysed the dust-corrected luminosity of the [O III] λ5007 line, Lum[O III]. We find that, in counter-rotating hosts, the AGN classified as Composite and Ambiguous have a slightly enhanced nuclear activity. Nevertheless, the median of the Lum[O III] values is almost identical (within the estimated errors) for Seyfert and LINER galaxies.

ACKNOWLEDGEMENTS

The authors thank Dr Xavier Hernandez for a detailed revision and useful comments.

This work was partially supported by the Consejo Nacional de Investigaciones Científicas y Técnicas and the Secretaría de Ciencia y Técnica de la Universidad Nacional de San Juan.

Funding for the SDSS has been provided by the Alfred P. Sloan Foundation, the Participating Institutions, the National Science Foundation, the US Department of Energy, the National Aeronautics and Space Administration, the Japanese Monbukagakusho, the

Max Planck Society and the Higher Education Funding Council for England. The SDSS website is http://www.sdss.org/.

The SDSS is managed by the Astrophysical Research Consortium for the Participating Institutions. The Participating Institutions are the American Museum of Natural History, Astrophysical Institute Potsdam, University of Basel, University of Cambridge, Case Western Reserve University, University of Chicago, Drexel University, Fermilab, the Institute for Advanced Study, the Japan Participation Group, Johns Hopkins University, the Joint Institute for Nuclear Astrophysics, the Kavli Institute for Particle Astrophysics and Cosmology, the Korean Scientist Group, the Chinese Academy of Sciences (LAMOST), Los Alamos National Laboratory, the Max-Planck-Institute for Astronomy (MPIA), the Max-Planck-Institute for Astrophysics (MPA), New Mexico State University, Ohio State University, University of Pittsburgh, University of Portsmouth, Princeton University, the United States Naval Observatory and the University of Washington.

REFERENCES

Abazajian K. N. et al., 2009, ApJS, 182, 543
Alonso M. S., Lambas D. G., Tissera P. B., Coldwell G., 2006, MNRAS, 367, 1029
Alonso S., Mesa V., Padilla N., Lambas D. G., 2012, A&A, 539, A46
Baldwin J. A., Phillips M. M., Terlevich R., 1981, PASP, 93, 5 (BPT)
Balogh M., Morris S. L., Yee H. K. C., Carlberg R. G., Ellingson E., 1999, ApJ, 527, 54
Balogh M., Baldry I. K., Nichol R., Miller C., Bower R., Glazebrook K., 2004, ApJ, 615, L101
Barton E. J., Geller M. J., Kenyon S. J., 2000, ApJ, 530, 660
Blanton M. R., Roweis S., 2007, AJ, 133, 734
Blanton M. R., Lin H., Lupton R. H., Maley F. M., Young N., Zehavi I., Loveday J., 2003, AJ, 125, 2276
Brinchmann J., Chalot S., White S. D. M., Tremonti C., Kauffmann G., Heckman T., Brinkmann J., 2004, MNRAS, 351, 1151
Calzetti D., Armus L., Bohlin R. C., Kinney A. L., Koornneef J., Storchi-Bergmann T., 2000, ApJ, 533, 682
Cervantes-Sodi B., Hernandez X., Park C., 2010, MNRAS, 402, 1807
Cervantes-Sodi B., Hernandez X., Park C., Choi Y.-Y., 2011, ApJ, 735, L25
Charlton J., Knierman K., Hunsberger S., Gallagher S., Whitmore B., Kundu A., Hibbard J., 2000, in Livio M., Noll K., Stiavelli M., eds, Space Telescope Science Institute Symposium, A Decade of HST Science: Poster Papers. Space Telescope Science Institute, Baltimore, p. 20
Darg D. W. et al., 2010, MNRAS, 401, 1552
Deng X.-F., 2013, Res. Astron. Astrophys., 13, 651
Di Matteo P., Combes F., Melchior A.-L., Semelin B., 2007, A&A, 468, 61
Dubinski J., Mihos J. C., Hernquist L., 1996, ApJ, 462, 576
Efron B., 1979, Ann. Stat., 7, 1
Ellison S. L., Patton D. R., Simard L., McConnachie A. W., Baldry I. K., Mendel J. T., 2008, MNRAS, 407, 1514
Fukugita M., Ichikawa T., Gunn J. E., Doi M., Shimasaku K., Schneider D. P., 1996, AJ, 111, 1748
Gunn J. E. et al., 1998, AJ, 116, 3040
Heckman T. M., Kauffmann G., Brinchmann J., Charlot S., Tremonti C., White S. D. M., 2004, ApJ, 613, 109
Heckman T. M., Ptak A., Hornschemeier A., Kauffmann G., 2005, ApJ, 634, 161
Hernandez X., Lee W. H., 2004, MNRAS, 347, 1304
Hogg D. W., Blanton M. (SDSS Collaboration), 2001, BAAS, 34, 570
Hunsberger S. D., Charlton J. C., Zaritsky D., 1966, ApJ, 462, 50
Kauffmann G., White S. D. M., Guiderdoni B., 2002, MNRAS, 264, 201
Kauffmann G. et al., 2003a, MNRAS, 341, 33
Kauffmann G. et al., 2003b, MNRAS, 346, 1055
Kennicutt R., 1998, ARA &A, 36, 189
Kewley L. J., Dopita M. A., Sutherland R. S., Heisler C. A., Trevena J., 2001, ApJ, 556, 121
Kewley L. J., Groves B., Kauffmann G., Heckman T. M., 2006, MNRAS, 372, 961
Kormendy J., Norman C. A., 1979, ApJ, 233, 539
Lambas D. G., Tissera P. B., Alonso M. S., Coldwell G., 2003, MNRAS, 346, 1189
Lambas D. G., Alonso S., Mesa V., O'Mill A. L., 2012, A&A, 539, A45 (L12)
Liu X., Shen Y., Strauss M. A., 2012, ApJ, 745, 94
Mihos J. C., Hernquist L., 1994, ApJ, 431, L9
Mirabel I. F., Dottori H., Lutz D., 1992, A&A, 256, L19
Mohamed Y. H., Reshetnikov V. P., Sotnikova N. Ya., 2011, Astron. Lett., 37, 670
Mulchaey J. S., Koratkar A., Ward M. J., Wilson A. S., Whittle M., Antonucci R. R. J., Kinney A. L., Hurt T., 1994, ApJ, 436, 586
O'Mill A. L., Duplancic F., García Lambas D., Sodré L., 2011, MNRAS, 413, 1395
O'Mill A. L., Duplancic F., García Lambas D., Valotto C., Sodré L., 2012, MNRAS, 421, 1897
Osterbrock D. E., Miller J. S., 1989, Proc. IAU Symp. 134, Active Galactic Nuclei. Kluwer, Dordrecht, p. 134
Patton D. R., Ellison S. L., Simard L., McConnachie A. W., Mendel J. T., 2011, MNRAS, 412, 591
Pérez J., Tissera P., Padilla N., Alonso M. S., Lambas D. G., 2009, MNRAS, 399, 1157
Pier J. R., Munn J. A., Hindsley R. B., Hennessy G. S., Kent S. M., Lupton R. H., Ivezić Ž., 2003, AJ, 125, 1559
Reshetnikov V. P., Sotnikova N. Ya., 2001, Astron. Astrophys. Trans., 20, 111
Salim S. et al., 2007, ApJS, 173, 267
Scudder J. M., Ellison S. L., Torrey P., Patton D. R., Mendel J. T., 2012, MNRAS, 426, 549
Smith J. A., Tucker D. L., Allam S. S., Jorgensen A. M., 2002, BAAS, 34, 1272
Smith J. A., Giroux M. L., Struck C., Hancock M., Hurlock S., 2010, in Smith B., Bastian N., Higdon S. J. U., Higdon J. L., eds, ASP Conf. Ser. Vol. 423, Galaxy Wars: Stellar Populations and Star Formation in Interacting Galaxies. Astron. Soc. Pac., San Francisco, p. 257
Strateva I. et al., 2001, AJ, 122, 1861
Strauss M. A. et al., 2002, AJ, 124, 1810
Toomre A., Toomre J., 1972, ApJ, 178, 623
Tremonti C. et al., 2004, ApJ, 613, 898
Yamauchi C. et al., 2005, AJ, 130, 1545
Yee H. K. C., Ellingson E., 1995, ApJ, 445, 37
York D. G. et al., 2000, AJ, 120, 1579

This paper has been typeset from a TEX/LATEX file prepared by the author.